Studies of multi-channel spark ignition of lean n-pentane/air mixtures in a spherical chamber

Hao Zhao[1,*], Tianhan Zhang[1], Ningbo Zhao[1,2], Shuqun Wu[1,3], Guoming Ma[1,4], Chao Yan[1], Hongtao Zhong[1], Yiguang Ju[1]

[1]Department of Mechanical and Aerospace Engineering, Princeton University, Princeton, NJ 08544, USA

[2]College of Power and Energy Engineering, Harbin Engineering University, Harbin, 150001, China

[3]College of Automation Engineering, Nanjing University of Aeronautics and Astronautics, Nanjing 210016, China

[4]The State Key Laboratory of Alternate Electrical Power System with Renewable Energy Sources, North China Electric Power University, Beijing, 102206, China

[*]Corresponding author's email address: haozhao@princeton.edu

Abstract

A novel ignition strategy using multi-channel sparks was developed in this paper. Compared with the typical single spark, the three-channel spark ignition technique enables three spatially separated and temporally synchronized discharges to increase the ignition kernel size while maintaining the same total ignition energy. The three-channel discharge characteristics, ignition kernel development, and ignition probability of lean n-pentane/air mixtures were studied and compared with those of single-channel

spark in a spherical combustion chamber with different discharge distances, pressures, and CO_2 dilution levels. The experimental results show that the three-channel sparks increase the ignition probability and dramatically extend the fuel-lean ignition limits compared to the single-channel discharge under all tested conditions. Moreover, ignition enhancement effects of multi-channel sparks increase with the decrease of pressure, reduction of discharge gap, and increase of CO_2 dilution. One-dimensional numerical simulation was performed by using a detailed n-pentane kinetic model (Bugler, et al. 2017) and the results revealed that the increase of fuel lean ignition probability and the decrease of the minimum ignition energy by using multi-channel sparks were the outcome of increased ignition kernel size compared to the minimum critical ignition radius. This present study confirms the advantages of using multi-channel sparks on advanced fuel-lean combustion engines.

1. Introduction

Due to the needs of high efficiency and low emission in combustion engines, gas engines, and power plants [1-5], many advanced clean combustion techniques, such as twin annular premixing swirler (TAPS) [6], lean direct injection (LDI) [7], lean premixed prevaporized (LPP) [8], trapped vortex combustion (TVC) [9], flameless combustion (FC) [10, 11], ultralean gas engines, spark assisted homogenous charged compression ignition (SA-HCCI) engines, and exhaust gas recirculation (EGR) [12-14], have been studied in recent years. Particularly, the fuel-lean combustion strategy has gained increasing attention for its lower combustion temperature, higher combustion efficiency, and knocking resistance. However, reliable ignition is very challenging at the fuel-lean conditions due to the rapid increase of ignition energy [15]. Although multi-coil ignition techniques [16] have been developed to increase the ignition energy, reliability of ignition coils and erosion of electrodes at high spark energy remain be challenging issues.

The initial ignition kernel formation, ignition kernel growth, and flame acceleration after the ignition kernel size passing the critical ignition radius are three main phases of the spark ignition process [17-21]. In most spark-ignition combustors, the initial kernel is formed through a spark discharge between a pair of electrodes, and the initial energy deposited into the combustible mixture must be larger than the minimum ignition energy (MIE), which is governed by the critical ignition radius [19-23], to achieve a successful ignition. The effect of MIE on combustion ignition has been

studied in experiments [19-21, 24-27], theory [19], and simulations [20, 28, 29], where flame can only propagate when the flame kernel radius passes through the critical flame radius. However, compared to the fuel-rich conditions, at the fuel-lean conditions close to the ignition limit, the MIE grows dramatically due to the increase of Lewis number, and the increase of the discharge voltage has little effect on the ignition [30]. Moreover, the high discharge voltage shortens the lifetime of igniters significantly [31]. Therefore, many efforts have been made to reduce the MIE in combustors by using optimized electrode configurations that increase the ignition kernel size [32-34] such as radio frequency spark [30, 35], laser-induced spark [36-38], high frequency microwave [39-42], and nanosecond repetitively pulsed plasma [43- 45]. All of the above studies confirmed that the spark kernel volume affected the MIE dramatically, and the increased spark kernel volume could extend the ignition limit and improve the operating stability of engines. Meanwhile, the detailed experimental analysis in Yu. et al. [30] showed that under the same operating condition, the increase of discharge energy had limited effect on enhancing the initial flame growth and extending the ignition limits, while the multiple spark strategy had significant influence on the ignition process. Besides, by using the repetitive nanosecond pulsed discharge, Lefkowitz et al. [43-44] experimentally investigated the impact of the initial ignition radius on flame initiation in a high-speed turbulent flow. They observed that multiple overlapping pulse discharges enhanced the ignition probability with constant discharge energy. In addition, Lin et al. [45] compared the ignition behaviors of three discharge modes (spark, single-channel nanosecond discharge, and multi-channel nanosecond discharge) for premixed

Therefore, the goal of this study is to understand the role of the spark kernel volume in affecting combustion ignition with fixed total ignition energy by using multi-channel sparks. Firstly, a novel multi-channel spark system is designed to increase the spark kernel volume while maintaining constant discharge energy. The characteristics of discharge are compared between single-channel and multi-channel spark system. Secondly, the ignition kernel development and the ignition probability of lean n-pentane/air mixtures are studied between single-channel and multi-channel spark

system in a spherical combustion chamber under varied electrode distances, pressures, and CO_2 dilution levels. Finally, one-dimensional numerical simulations are performed to examine the mechanism of ignition enhancement by using the multi-channel spark system.

2. Experimental and numerical methods

2.1 Experimental setup

The experiments are conducted in a high-pressure constant-volume spherical chamber which has been successfully used and validated in previous studies [21, 25, 46-48]. As shown in Fig. 1 (a), it consists of a spherical chamber, an ignition system, and a pressure release system. At first, the chamber is evacuated and filled with a small amount of N_2 (99.9%) to avoid the trapping of fuel in crevices and pressure gauge lines. Then, the unburned gas reactant mixture is prepared by using the partial pressure method [21, 46, 49], and the pressure is measured by using a pressure gauge (Kulite XTEL-190) with 4 digit accuracy.
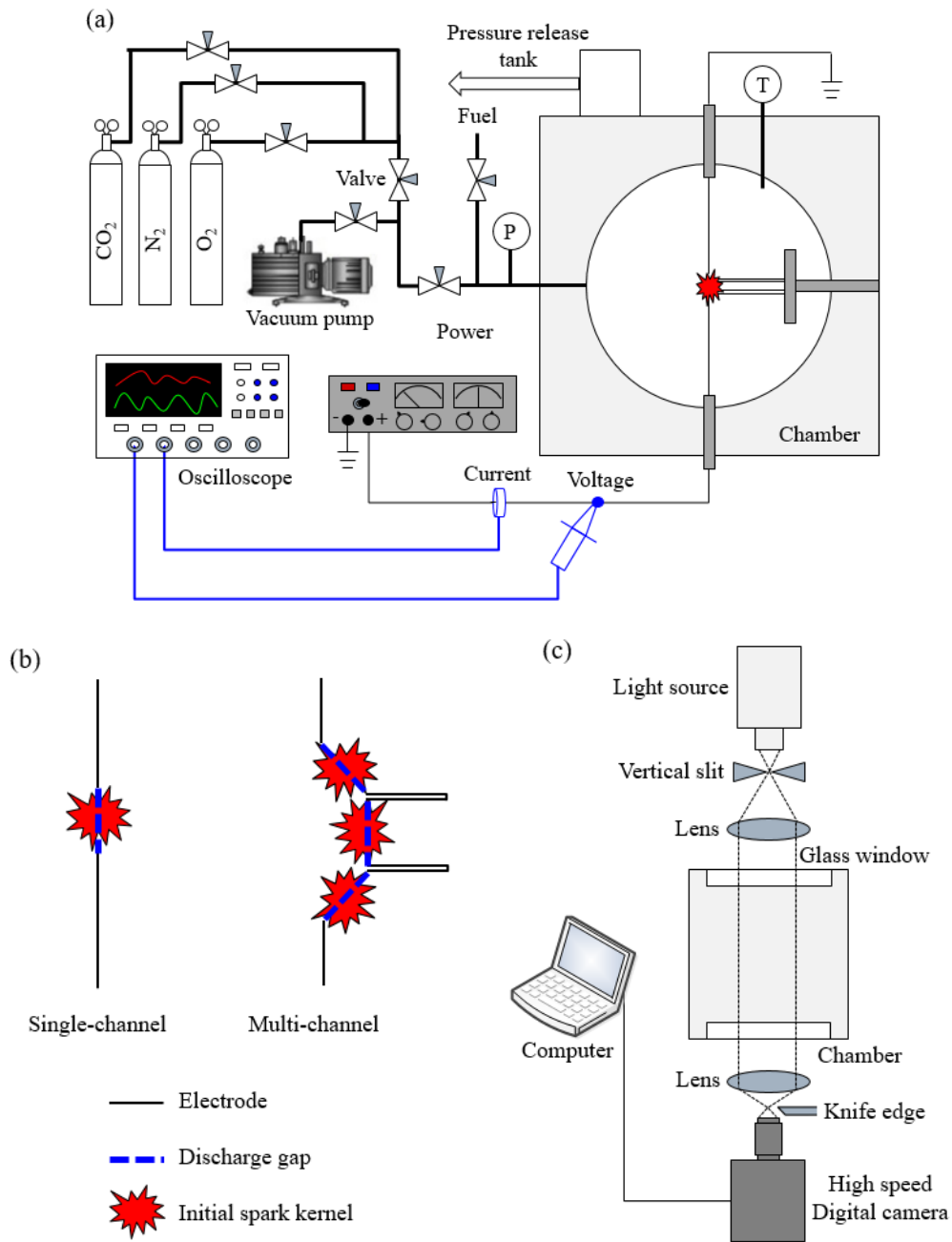
Fig. 1 Schematics of (a) experimental platform, (b) two configurations of spark discharge (single vs. multi-channel), and (c) schlieren imaging

For the ignition system, Fig. 1 (b) shows two types of electrode configurations which are used to investigate the effects of the initial ignition kernel volume and ignition geometry on the ignition process. One is the conventional single-channel configuration which includes a pair of electrodes, respectively, installed at the top and

bottom of the chamber. The diameter of electrodes is about 1mm. The upper electrode is mounted with a linear translation stage to control the distance between the electrodes. Another is the newly designed multi-channel configuration which has three discharge channels in a triangle ignition geometry to increase the ignition kernel size. The multi-channel discharge only has one power supply and three simultaneous discharges are triggered by a special circuit. All the electrodes are on the same vertical plane and are symmetric along the X-Y plane, and three spark discharges are generated between two electrodes with the same predetermined constant gap distance. The single-channel and multi-channel configurations can be easily switched by controlling the position of the upper electrode. During the discharge process, the voltage and current traces are measured by using a high voltage probe (LeCroy, PPE20KV) and a Pearson Coil (Model 6585), respectively. The waveforms are recorded by a digital phosphor oscilloscope (Tektronix DPO7104C).

After the central ignition of the quiescent combustible mixture, the unsteady flame propagation is recorded by using a high-speed schlieren imaging method (Fig. 1 (c)) at a frame rate of 10,000/s and image resolution of 1024×1024. The major source of the ignition and flame speed uncertainty is the fuel concentration at fuel lean conditions due to the partial pressure method. Calculated from the root-mean-square sum of the uncertainties from different sources, the total uncertainty of this study is within 5%. More details of the experimental uncertainties are described elsewhere [21].

As shown in Table 1, the ignition experiments of n-pentane/air mixtures in the single-channel and the multi-channel electrode configurations are conducted under

varied electrode separation distances, pressures, and CO_2 dilution levels.

Table 1 Experimental conditions for n-pentane/air mixtures.

Case	Electrode gap distance (mm)	Pressure (atm)	Equivalence ratio	CO_2 dilution (% in mole)
1	2.5	1	0.60-0.80	0
2	2.5	0.5	0.60-0.80	0
3	2.5	1	0.60-0.80	20
4	1	1	0.60-0.80	20
5	1	3	0.60-0.80	20

2.2 Numerical model

A one-dimensional transient compressible flow solver for Adaptive Simulation of Unsteady Reactive Flow (ASURF+) is utilized to simulate the ignition and flame propagation processes. ASURF+ has been validated in a series of studies on ignition, unsteady flame propagation, and detonation [19, 20, 28, 29, 50]. The details of ASURF+ solver and the governing equations, numerical methods, boundary conditions, and code validations can be found in [19]. The computation is conducted in the spherical coordinate system and the domain size ranges from 1 to 4cm. Multi-level adaptive grids are used near the flame front. The smallest grid size is 20μm, and the timestep is 10ns. The ignition kernel is initialized by a high temperature kernel. The reduced n-pentane/air combustion reaction mechanism developed by Bugler et al. [51] is employed in the simulation.

3. Results and discussions

3.1 Discharge characteristics in air for different electrode configurations

The measured voltage and current profiles in the single-channel and the multi-channel electrode discharges in air are shown in Fig. 2 (a) and (b), respectively, with a data sampling interval of 1ns. It is clearly seen that under the same experimental condition, the single- and multi-channel electrode configurations exhibit very similar voltage and current time dependence, and the total integrated discharge energies for both systems are around 0.35mJ. Besides, according to Fig. 2 (a) and (b), the discharges of the single- and multi-channel electrode systems mainly consist of three stages: electrical breakdown stage, arc stage, and glow stage [52]. In the breakdown stage (about 1-5ns in Fig. 2), the narrow plasma channel between the electrode gap results in a rapid decrease of resistance and an increase of current with little energy loss. During the subsequent arc formation stage (6-400ns in Fig. 2), with the enhancement of plasma strength, the plasma channel rapidly transforms to an arc [45]. As a result, both of the electrical currents of the single-channel and the multi-channel electrode configurations reach the first peak value at the same time (around t = 16ns in Fig. 2), while the peak value of the latter is slightly smaller than the former due to the higher resistance with more electrode pairs in the multi-channel discharge configuration. At the glow stage (400-500ns in Fig. 2), most of the discharge energy is dissipated though the oscillating attenuation of current and voltage [52, 53]. The comparison between Fig. 2 (a) and (b) confirms that the both electrode configurations maintain the same total discharge energy and similar discharge voltage and current time histories, which enables the present study to isolate the effect of the spark kernel volume on the ignition process.
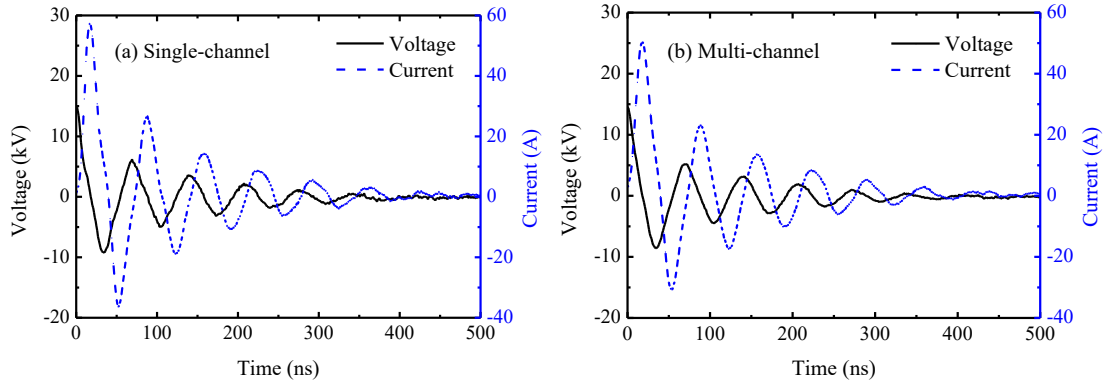
Fig. 2 The measured voltages and currents of (a) the single-channel and (b) the multi-channel electrode configurations as a function of time.

3.2 Effect of electrode configurations on ignition kernel evolution

Fig. 3 shows the high-speed shadowgraphs of the single-channel and multi-channel spark evolutions of an n-pentane/air mixture at equivalence ratio (*ER*) of 0.68. Pressure (*P*) is 0.5 atm, and discharge gap (*L*) between one pair of the electrodes in both the single-channel and the multi-channel spark configurations is 2.5mm. The time history of flame radius data and the burning velocity with stretch are collected with an automatic flame-edge detection and circle-fitting program of MATLAB, and are plotted in Fig. 4 (a) and (b), respectively. Both figures show that, at the same ignition energy (IE) and operating conditions, the multi-channel electrode configuration ignites the n-pentane/air lean mixture successfully, while the single-channel configuration fails due to the smaller ignition kernel size. It is also noticed from Fig. 3 (c) and Fig. 4 that for the single-channel ignition, the same n-pentane/air mixture still fails to be ignited with 2 times of ignition energy (0.7mJ) or longer discharge time, which is corresponding with Yu, et al. [30]. The comparison in Fig. 3 and 4 clearly indicates that the increase of the ignition kernel volume extends the ignition limit at the given ignition energy,

11

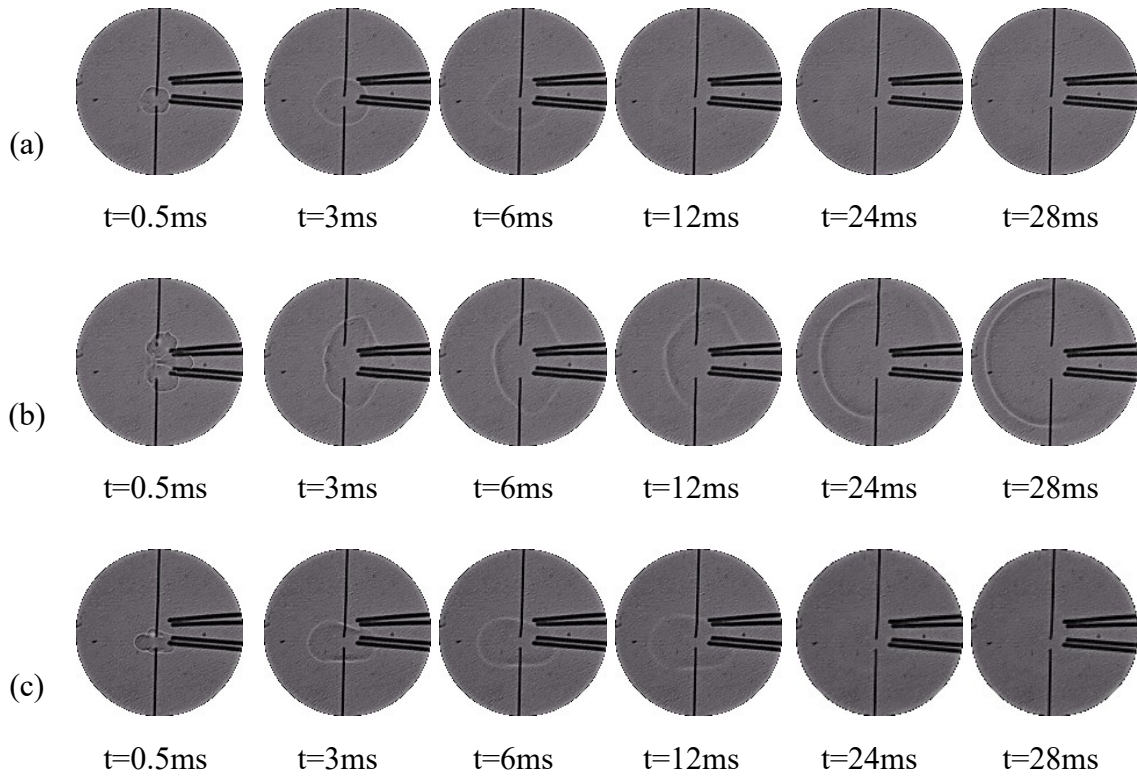where the enhancement of ignition energy has limited effects.

Fig. 3 Schlieren images of ignition kernel induced by (a) single-channel (0.35mJ) and (b) multi-channel (0.35mJ), and (c) single-channel (0.7mJ) electrode configurations for n-pentane/air mixture at $ER = 0.68$, $P = 0.5$ atm, and $L = 2.5$mm.
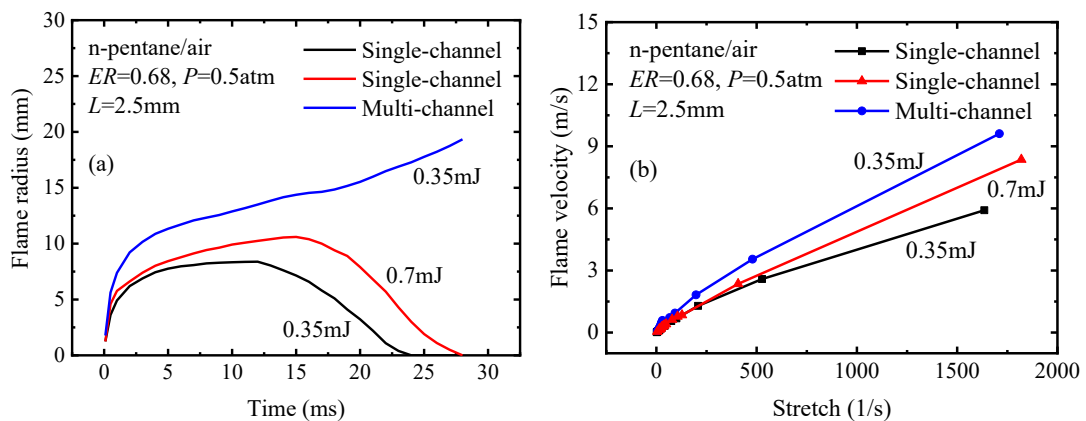

Fig. 4 (a) The measured flame radius as a function of time (a) and the burning velocity as a function of stretch (b) in single-channel (0.35mJ, 0.7mJ) and multi-channel (0.35mJ)

spark ignitions for n-pentane/air mixture at $ER = 0.68$, $P = 0.5$ atm, and $L = 2.5$mm.

3.3 Ignition probability enhancement by multi-channel electrode configuration under various experimental conditions

In order to comprehensively understand the effect of the spark kernel volume on ignition, many ignition experiments at different equivalence ratios, pressures, electrode gap distance and CO_2 additions levels (Table 1) are performed and compared. In addition, the ignition probability [44] is used to quantify the ignition performance of the single-channel and the multi-channel electrode configurations. The ignition probability is defined as the ratio between the number of the successful ignitions and the total number of trials. Ten trials are performed for each condition in the present experiments.

Fig. 5 depicts the ignition probabilities of the single-channel and the multi-channel ignition systems for n-pentane/air mixtures at different pressures (case 1 and 2 in Table 1). It is seen that, as is expected, the ignition probabilities of both of single-channel and the multi-channel discharges reduce quickly as the equivalence ratio decreases in Fig. 5 (a) and (b). Moreover, at the same equivalence ratio, the ignition probability of the multi-channel discharge is obviously higher than that of the single-channel one at the same ignition energy. The results show that the leaner the mixture is, the larger ignition enhancement the multi-channel ignition system has. As a result, the lean ignition limit is effectively extended with the multi-channel spark ignition system. For example, at 0.5 atm in Fig. 5 (b), the lean ignition limit for 100% successful ignition (the ignition probability = 1) is extended from ER of 0.76 to 0.68. In addition, an evaluation

13

parameter, ignition enhancement, is used to assess the ignition improvement of the multi-channel discharge over the single-channel discharge. It is defined as the area between the two ignition probability curves of multi-channel discharge and the single-channel discharge in Fig. 5 (a) and (b). It is seen that the ignition enhancement at 0.5 atm in Fig. 5 (b) is larger than at 1 atm in Fig. 5 (a). In another word, the ignition enhancement of multi-channel sparks is more obvious at lower pressures. That is because the critical ignition radius increases with the decrease of the pressure. As a result, the mixture requires a larger spark kernel volume for successful ignition at lower pressures.
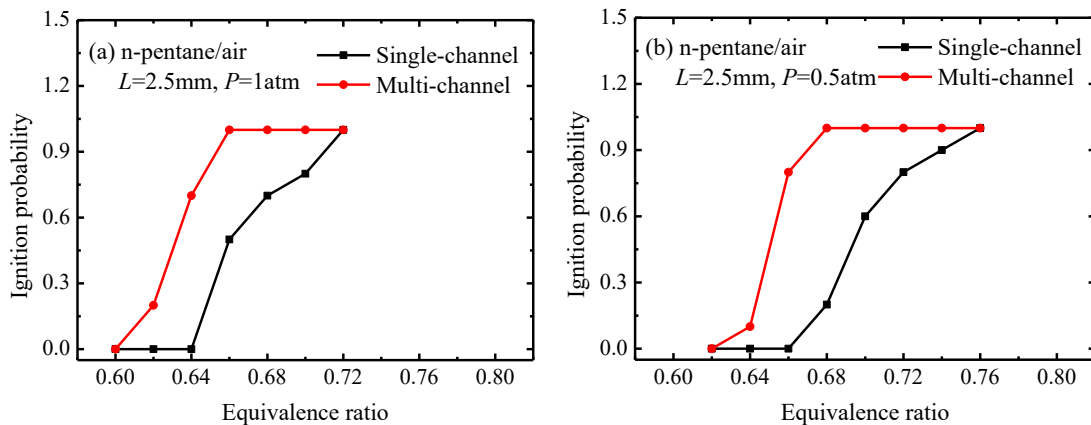

Fig. 5 Ignition probability as a function of equivalence ratio for the n-pentane/air mixture at $L = 2.5$ mm: (a) $P = 1$ atm and (b) $P = 0.5$ atm.

Fig. 6 shows the ignition probability profile of the lean n-pentane/air/20%CO_2 mixture using the two different ignition systems under different pressures and electrode separation distances. All of the experimental results in Fig. 5 (a-b) and 6 (a-c) show that the multi-channel spark has a higher ignition probability and extends the ignition limit of the single-channel spark at different pressures, electrode separation distances, and CO_2 addition levels.

Compared with Fig. 5 (a), 20% CO_2 is added in Fig. 6 (a) to study the effect of the two electrode separation distances with/without CO_2 additions from EGR on the ignition probabilities, while maintaining the same adiabatic flame temperature. Note that the addition of CO_2 dilution significantly deteriorates the ignition process of both the single-channel and the multi-channel discharges mainly due to the increase of activation energy and slowdown of chain-branching reactions with CO_2 dilution. For example, by adding 20% CO_2, the lean ignition limit for completely successful ignition (the ignition probability = 1) changes from equivalence ratio of 0.66 to 0.7 in the multi-channel discharge. Nevertheless, the ignition enhancement in Fig. 6 (a) is larger than that in Fig. 5 (a), indicating an improved effect of the multi-channel spark ignition system on the ignition when EGR is included.

It is seen from Fig. 6 (a) and (b) that the decrease of electrode separation distance reduces the ignition probability for both ignition systems. Also, the results show that there is an improved effect of the multi-channel spark system on the ignition with a smaller discharge gap (ignition enhancement in Fig. 6 (b) is larger than that in Fig. 6 (a)).

The comparison between Fig. 6 (b) and (c) further demonstrates the effectiveness of the multi-channel sparks at different pressures. It is seen that the ignition enhancement at 1 atm in Fig. 6 (b) is larger than that at 3atm in Fig. 6 (c), which confirms that the multi-channel sparks is more effective at lower pressures and fuel lean conditions where the critical ignition radius is larger [19, 28].
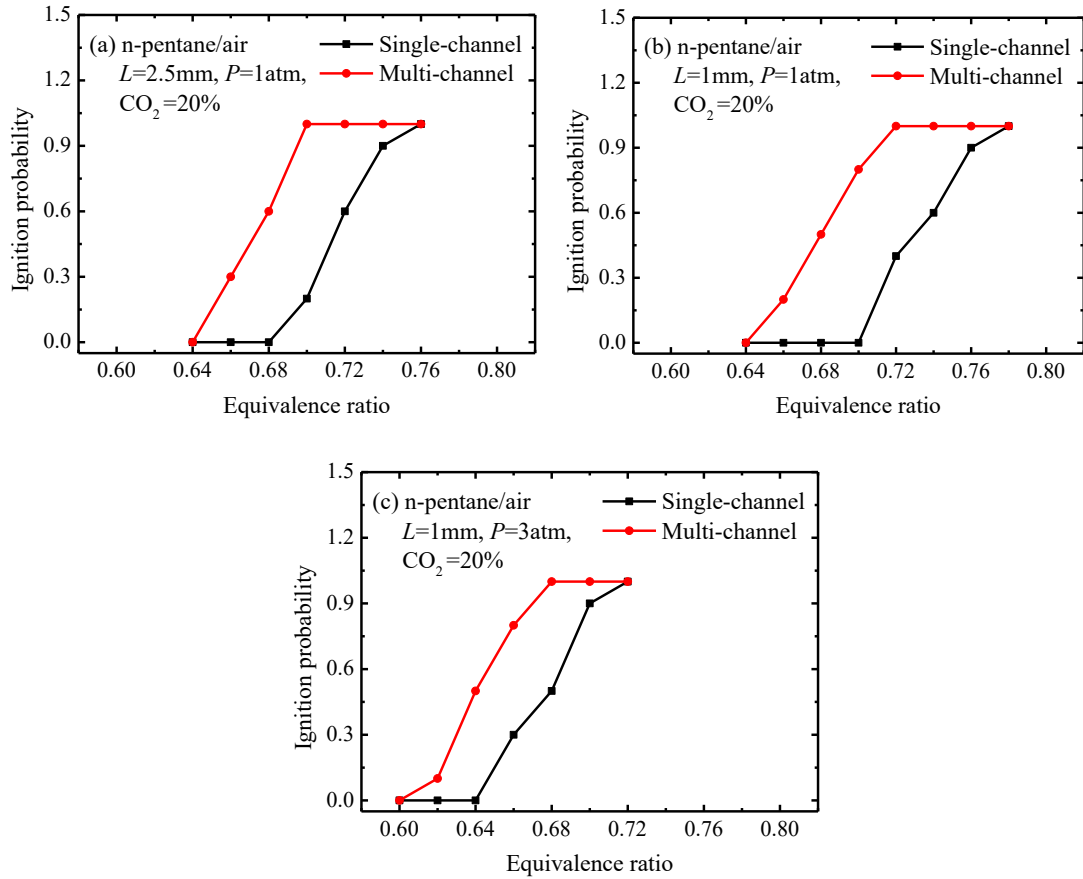
Fig. 6 Ignition probability as a function of equivalence ratio for the n-pentane/air/20% CO_2 mixture at: (a) $L = 2.5$mm, $P = 1$atm, (b) $L = 1$mm, $P = 1$atm, and (c) $L = 1$mm, $P = 3$atm.

3.4 Simulations of ignition enhancement mechanism

In order to better understand the effect of the initial ignition kernel size on successful ignition of fuel lean mixtures by using the multi-channel spark system, several numerical simulations were performed to simulate one-dimensional outwardly propagating spherical flames initiated by different types of initial flame kernel volume for n-pentane/air mixture at $ER = 0.68$ and $P = 0.5$ atm.
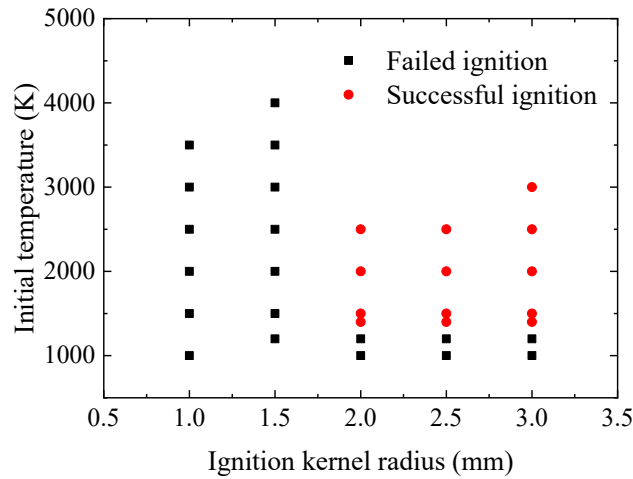
Fig. 7 Summary of ignition success and failure of single-channel spark ignition at different ignition kernel radiuses and initial ignition kernel temperature (ignition energy).

Fig. 7 shows the summary of the simulation results for the single-channel spark ignitions with different ignition kernel radiuses and initial kernel temperatures. The model assumes the ignition spark creates a high temperature sphere in the center of the combustion chamber and ignites the mixture. An ignition failure means that the initial ignition kernel will extinguish as the flame radius increase and fails to produce a quasi-steady outwardly propagating spherical flame. It can be clearly seen in Fig.7 that both low ignition temperature (ignition energy) and small ignition kernel size affect the failure of ignition. At a large electrode separation distance, ignition energy plays an important role. However, at a small electrode separation distance, the ignition energy required for successful ignition increases dramatically. Therefore, for very lean mixtures where the critical radius is large, increasing the ignition kernel size using a multi-spark ignition system is more effective than increasing the ignition energy using a single spark ignition system. This is consistent with our experimental observations. From our experimental observation in the multi-channel spark cases, the three ignition kernels merge with each other and form a much larger ignition kernel size at a very

early ignition stage (~0.5ms) to enhance the ignition.

To demonstrate the mechanism of increased ignition kernel size using the multi-channel spark ignition system and simplify the simulations, the three-dimensional multi-channel ignition kernels are modeled as a one-dimensional spherical shell. The initial condition of the multi-channel spark modeling is as followed. The inner radius of the merged shell is 3mm in corresponding with the observed shell in the experiment, and the shell thickness is 0.5mm. The initial temperature is 1800K. For the single-channel spark case, a solid sphere is employed with the spark radius of 1.5mm and temperature of 2500K, which keeps the same ignition energy with the multi-channel spark case. Note that the single-channel spark at this condition fails to ignite the mixture, while the multi-spark ignition shell with increased ignition volume at the same ignition energy (Fig. 8) ignites the mixture and results in an outwardly propagating spherical flame at time of 20ms. The present simplified simulation confirms that with a fixed ignition energy, a larger ignition kernel size by the multi-spark ignition system helps to drive the flame kernel to exceed the critical ignition radius and thus extends the lean ignition limits of a fuel lean mixture.
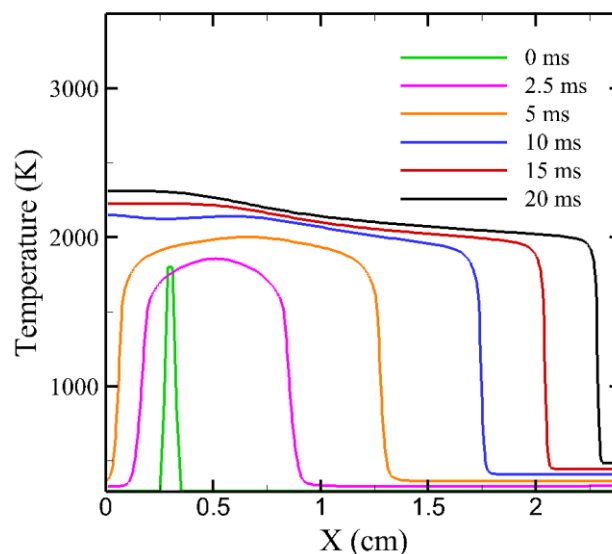

Fig. 8 Simulation results of the temporal evolution of temperature distribution for the

multi-channel ignition system using an ignition shell. The initial inner radius of the ignition shell is 3mm, the shell thickness 0.5mm, the initial temperature 1800K, pressure P = 0.5 atm, and equivalence ratio Φ = 0.68.

4. Conclusions

In this paper, a novel multi-channel spark ignition system has been developed. It enables three spatially separated and temporally synchronized discharges to increase the ignition kernel size while maintaining the same total ignition energy. Experiments and numerical simulations were carried out to understand the role of the increased initial spark kernel volume by the multi-channel spark ignition system in affecting the ignition probability of lean n-pentane/air mixture at varied electrode separation distances, pressures, and CO_2 dilution levels, compared to the single channel ignition system. From this work, the following conclusions nay be drawn:

(1) The novel multi-channel spark ignition technique can generate a larger ignition kernel than the traditional single-channel discharge at the same total ignition energy. The increased ignition kernel size significantly extends the lean ignition limits of n-pentane/air mixtures.

(2) At lower pressures, leaner fuel mixtures, and higher CO_2 dilution levels in which the critical ignition radius increases, the effectiveness of the multi-channel spark ignition system in enhancing ignition increases. Moreover, the results show that the smaller the electrode separation distance is, the more effective the multi-channel spark ignition system is in increasing the ignition probability.

(3) One-dimensional simulations show that both ignition energy and initial ignition kernel size affect ignition probability. At a large electrode separation distance, ignition energy plays an important role. However, at a small electrode separation distance, the ignition energy required for successful ignition increases dramatically.   Therefore, for very lean mixtures with large critical ignition radius, increasing the ignition kernel size using a multi-spark ignition system is more effective than increasing the ignition energy using a single spark ignition system. This result is consistent with the present experimental observations.

The present study reveals a great potential of applying the multi-channel spark technique on advanced fuel-lean combustion engines.

Conflict of interest

We declare that we have no conflict of interest.

Acknowledgments

References

[1] M. Suresh, C.P. Jawahar, A. Richard, A review on biodiesel production, combustion, performance, and emission characteristics of non-edible oils in variable compression ratio diesel engine using biodiesel and its blends, Renew. Sust. Energ. Rev. 92 (2018) 38-49.

[2] P. Kyrtatos, A. Zivolic, C. Brückner, K. Boulouchos, Cycle-to-cycle variations of NO emissions in diesel engines under long ignition delay conditions, Combust. Flame 178 (2017) 82-96.

[3] M.A. Nemitallah, S.S. Rashwan, I.B. Mansir, A.A. Abdelhafez, M.A. Habib, Review of novel combustion techniques for clean power production in gas turbines, Energ. Fuel. 32 (2018) 979-1004.

[4] Z. Zhang, H. Zhao, L. Cao, G. Li, Y. Ju, Kinetic effects of n-heptane addition on low and high temperature oxidation of methane in a jet-stirred reactor, Energ. Fuel. 32 (2018) 11970-11978.

[5] H. Zhao, G. Song, L. Shen, Y. Yu, Novel technique route of coal gasification with CO_2 capture using CaO sorbents via three-stage interconnected fluidized beds. Energ. Fuel. 26 (2012) 2934-2941.

[6] M. Foust, D. Thomsen, R. Stickles, C. Cooper, W. Dodds, Development of the GE aviation low emissions TAPS combustor for next generation aircraft engines, 50th AIAA Aerospace Sciences Meeting including the New Horizons Forum and Aerospace Exposition (2012), paper AIAA2012-0936.

[7] V. Deepika, S.R. Chakravarthy, T.M. Muruganandam, N.R. Bharathi, Multi-swirl lean direct injection burner for enhanced combustion stability and low pollutant emissions, ASME 2017 Gas Turbine India Conference (2017), paper GTINDIA2017-4905.

[8] P. Gokulakrishnan, M.J. Ramotowski, G. Gaines, C. Fuller, R. Joklik, L.D. Eskin, M.S. Klassen, R.J. Roby, A novel low NOx lean, premixed, and prevaporized combustion system for liquid fuels, J. Eng. Gas Turbines Power 130 (2008) 051501.

[9] D. Zhao, E. Gutmark, P.D. Goey, A review of cavity-based trapped vortex, ultra-compact, high-g, inter-turbine combustors, Prog. Energy Combust. Sci. 66 (2018)

42-82.

[10] A.A.V. Perpignan, A.G. Rao, D.J.E.M. Roekaerts, Flameless combustion and its potential towards gas turbines, Prog. Energy Combust. Sci. 69 (2018) 28-62.

[11] K.I. Khidr, Y.A. Eldrainy, M.M. EL-Kassaby, Towards lower gas turbine emissions: Flameless distributed combustion, Renew. Sust. Energ. Rev. 67 (2017) 1237-1266.

[12] K. Cung, A.A. Moiz, X. Zhu, S.Y. Lee, Ignition and formaldehyde formation in dimethyl ether (DME) reacting spray under various EGR levels, Proceed. Combust. Inst. 36 (2017) 3605-3612.

[13] L. Cai, A. Ramalingam, H. Minwegen, K.A. Heufer, H. Pitsch, Impact of exhaust gas recirculation on ignition delay times of gasoline fuel: An experimental and modeling study, Proceed. Combust. Inst. 37 (2018) 639-647.

[14] H. Zhao, A.G. Dana, Z. Zhang, W.H. Green, Y. Ju, Experimental and modeling study of the mutual oxidation of n-pentane and nitrogen dioxide at low and high temperatures in a jet stirred reactor, Energy 165 (2018) 727-738.

[15] D. Jung, K. Sasaki, T. Yokomori, N. Iida, Influence of spark discharge energy and duration on cycle-to-cycle variations of SI combustion at lean limits, International symposium on diagnostics and modeling of combustion in internal combustion engines (2017), paper B309.

[16] D. Jung, N. Iida, An investigation of multiple spark discharge using multi-coil ignition system for improving thermal efficiency of lean SI engine operation, Appl. Energ. 212 (2018) 322-332.

[17] T. Jaravel, J. Labahn, B. Sforzo, J. Seitzman, M. Ihme, Numerical study of the ignition behavior of a post-discharge kernel in a turbulent stratified crossflow, Proceed. Combust. Inst. 37 (2019) 5065-5072.

[18] E. Mastorakos, Forced ignition of turbulent spray flames, Proceed. Combust. Inst. 36 (2017) 2367-2383.

[19] Z. Chen, Y. Ju, Theoretical analysis of the evolution from ignition kernel to flame ball and planar flame, Combust. Theory Model. 11 (2007) 427-453.

[20] Z. Chen, M.P. Burke, Y. Ju, On the critical flame radius and minimum ignition energy for spherical flame initiation, Proceed. Combust. Inst. 1 (2011) 1219-1226.

[21] H.H. Kim, S.H. Won, J. Santner, Z. Chen, Y. Ju, Measurements of the critical initiation radius and unsteady propagation of n-decane/air premixed flames, Proceed. Combust. Inst. 34(2013) 929-936.

[22] L.J. Jiang, S.S. Shy, M.T. Nguyen, S.Y. Huang, Spark ignition probability and minimum ignition energy transition of the lean iso-octane/air mixture in premixed turbulent combustion, Combust. Flame 187 (2018) 87-95.

[23] M. Zhou, G. Li, Z. Zhang, J. Liang, L. Tian, Effect of ignition energy on the initial propagation of ethanol/air laminar premixed flames: An experimental study, Energ. Fuel. 31 (2017) 10023-10031.

[24] A.P. Kelley, G. Jomaas, C.K. Law, Critical radius for sustained propagation of spark-ignited spherical flames, Combust. Flame 156 (2009) 1006-1013.

[25] J.S. Santner, S.H. Won, Y. Ju, Chemistry and transport effects on critical flame initiation radius for alkanes and aromatic fuels, Proceed. Combust. Inst. 36 (2017) 1457-1465.

[26] S.S. Shy, Y.W. Shiu, L.J. Jiang, C.C. Liu, S. Minaev, Measurement and scaling of minimum ignition energy transition for spark ignition in intense isotropic turbulence from 1 to 5 atm, Proceed. Combust. Inst. 36 (2017) 1785-1791.

[27] G. Cui, S. Wang, Z. Bi, Z. Li, Minimum ignition energy for the $CH_4/CO_2/O_2$ system at low initial temperature, Fuel 233 (2018) 159-165.

[28] Z. Chen, M.P. Burke, Y. Ju, Effects of Lewis number and ignition energy on the determination of laminar flame speed using propagating spherical flames, Proceed. Combust. Inst. 32 (2009) 1253-1260.

[29] Y. Wang, W. Han, Z. Chen, Effects of fuel stratification on ignition kernel development and minimum ignition energy of n-decane/air mixtures, Proceed. Combust. Inst. 37(2019) 1623-1630.

[30] S. Yu, M. Wang, M. Zheng, Distributed electrical discharge to improve the ignition of premixed quiescent and turbulent mixtures, SAE 2016 World Congress and Exhibition (2016), paper 2016-01-0706.

[31] H. M. Cho, B.Q. He, Spark ignition natural gas engines-A review, Energ. Convers. Manage. 48 (2007) 608-618.

[32] R.C. Meyer, D.P. Meyers, S.R. King, W.E. Liss, Effects of spark plug number and location in natural gas engines, J. Eng. Gas Turbines Power 114 (1992) 475-479.

[33] T. Badawy, X.C. Bao, H. Xu, Impact of spark plug gap on flame kernel propagation and engine performance, Appl. Energ. 191 (2017) 311-327.

[34] K. Xie, S. Yu, X. Yu, G. Bryden, M. Zheng, M. Liu, Investigation of multi-pole spark ignition under lean conditions and with EGR, SAE 2017 World Congress Experience (2017), paper 2017-01-0679.

[35] A. Mariani, F. Foucher, Radio frequency spark plug: An ignition system for modern internal combustion engines, Appl. Energ. 122 (2014) 151-161.

[36] I.A. Mulla, S.R. Chakravarthy, N. Swaminathan, R. Balachandran, Evolution of flame-kernel in laser-induced spark ignited mixtures: A parametric study, Combust. Flame 164 (2016) 303-318.

[37] T. Endo, K. Kuwamoto, W. Kim, T. Johzaki, D. Shimokuri, S.I. Namba, Comparative study of laser ignition and spark-plug ignition in high-speed flows,

Combust. Flame 191 (2018) 408-416.

[38] X. Bao, A. Sahu, Y. Jiang, T. Badawy, H. Xu, Flame kernel evolution and shock wave propagation with laser ignition in ethanol-air mixtures, Appl. Energ. 233 (2019) 86-98.

[39] B. Wolk, A. DeFilippo, J.Y. Chen, R. Dibble, A. Nishiyama, Y. Ikeda, Enhancement of flame development by microwave-assisted spark ignition in constant volume combustion chamber, Combust. Flame 160 (2013) 1225-1234.

[40] Z. Wang, J. Huang, Q. Wang, L. Hou, G. Zhang, Experimental study of microwave resonance plasma ignition of methane-air mixture in a constant volume cylinder, Combust. Flame 162 (2015) 2561-2568.

[41] J. Hwang, C. Bae, J. Park, W. Choe, J. Cha, S. Woo, Microwave-assisted plasma ignition in a constant volume combustion chamber, Combust. Flame 167 (2016) 86-96.

[42] M.K. Le, A. Nishiyama, T. Serizawa, Y. Ikeda, Applications of a multi-point microwave discharge igniter in a multi-cylinder gasoline engine, Proceed. Combust. Inst. 37 (2019) 5621-5628.

[43] J.K. Lefkowitz, P. Guo, T. Ombrello, S.H. Won, C.A. Stevens, J.L. Hoke, F. Schauer, Y. Ju, Schlieren imaging and pulsed detonation engine testing of ignition by a nanosecond repetitively pulsed discharge, Combust. Flame 162 (2015) 2496-2507.

[44] J.K. Lefkowitz, T. Ombrello, An exploration of inter-pulse coupling in nanosecond pulsed high frequency discharge ignition, Combust. Flame 180 (2017) 136-147.

[45] B.X. Lin, Y. Wu, Z.B. Zhang, Z. Chen, Multi-channel nanosecond discharge plasma ignition of premixed propane/air under normal and sub-atmospheric

pressures. Combust. Flame 182 (2017) 102-113.

[46] H. Zhao, J. Fu, F.M. Haas, Y. Ju, Effect of prompt dissociation of formyl radical on 1, 3, 5-trioxane and CH_2O laminar flame speeds with CO_2 dilution at elevated pressure, Combust. Flame 183 (2017) 253-260.

[47] D. Felsmann, H. Zhao, Q. Wang, I. Graf, T. Tan, X. Yang, E.A. Carter, Y. Ju, K. Kohse-Höinghaus, Contributions to improving small ester combustion chemistry: Theory, model and experiments, Proceed. Combust. Inst. 36 (2017) 543-551.

[48] H. Zhao, Z. Zhang, Y. Rezgui, N. Zhao, Y. Ju, Studies of high pressure 1,3-butadiene flame speeds and high temperature kinetics using hydrogen and oxygen sensitization, Combust. Flame 200 (2019) 135-141.

[49] L.S. Tran, J. Pieper, H.H. Carstensen, H. Zhao, I. Graf, Y. Ju, F. Qi, K. Kohse-Höinghaus, Experimental and kinetic modeling study of diethyl ether flames, Proceed. Combust. Inst. 36 (2017) 1165-1173.

[50] W. Liang, C.K. Law, Z. Chen, Ignition of hydrogen/air mixtures by a heated kernel: Role of Soret diffusion, Combust. Flame 197 (2018) 416-422.

[51] J. Bugler, A. Rodriguez, O. Herbinet, F. Battin-Leclerc, C. Togbé, G. Dayma, P. Dagaut, H.J. Curran, An experimental and modelling study of n-pentane oxidation in two jet-stirred reactors: The importance of pressure-dependent kinetics and new reaction pathways, Proceed. Combust. Inst. 36 (2017) 441-448.

[52] R. Maly, M. Vogel, Initiation and propagation of flame fronts in lean CH_4-air mixtures by the three modes of the ignition spark, Symp. (Int.) Combust. 17 (1979) 821-831.

[53] K. Eisazadeh-Far, F. Parsinejad, H. Metghalchi, J.C. Keck, On flame kernel formation and propagation in premixed gases, Combust. Flame 157 (2010) 2211-2221.